JGR Planets

RESEARCH ARTICLE
10.1029/2022JE007627

Compositional Variability of 2.0-Ga Lunar Basalts at the Chang'e-5 Landing Site

Samuele Boschi[1], Xiao-Lei Wang[1], Hejiu Hui[2,3], Zongjun Yin[4], Yue Guan[1], Huan Hu[1], Wenlan Zhang[1], Jiayang Chen[1], and Weiqiang Li[1,2,3]

[1]State Key Laboratory for Mineral Deposits Research, School of Earth Sciences and Engineering, Nanjing University, Nanjing, China, [2]School of Earth Sciences and Engineering, Lunar and Planetary Science Institute, Nanjing University, Nanjing, China, [3]CAS Center for Excellence in Comparative Planetology, Hefei, China, [4]State Key Laboratory of Palaeobiology and Stratigraphy, Nanjing Institute of Geology and Palaeontology, Chinese Academy of Sciences, Nanjing, China

Key Points:

- A new processing method of lunar rock clast is given to characterize the composition and age at milligram-level sample consumption
- An independent high-precision in situ secondary ion mass spectrometer Pb-Pb age of 2,040 ± 22 Ma is determined for a basaltic clast from the Chang'e-5 lunar mission
- The basaltic clasts returned by Chang'e-5 mission have remarkable compositional variability and are likely composed of low-Ti mare basalt

Supporting Information:

Supporting Information may be found in the online version of this article.

Correspondence to:

W. Li,
liweiqiang@nju.edu.cn

Citation:

Boschi, S., Wang, X.-L., Hui, H., Yin, Z., Guan, Y., Hu, H., et al. (2023). Compositional variability of 2.0-Ga lunar basalts at the Chang'e-5 landing site. *Journal of Geophysical Research: Planets*, *128*, e2022JE007627. https://doi.org/10.1029/2022JE007627

Received 18 OCT 2022
Accepted 4 MAY 2023

Author Contributions:

Conceptualization: Weiqiang Li
Funding acquisition: Weiqiang Li
Investigation: Samuele Boschi, Jiayang Chen, Weiqiang Li
Methodology: Samuele Boschi, Xiao-Lei Wang, Zongjun Yin, Yue Guan, Huan Hu, Wenlan Zhang, Weiqiang Li
Project Administration: Weiqiang Li
Resources: Xiao-Lei Wang, Weiqiang Li
Supervision: Weiqiang Li
Writing – original draft: Samuele Boschi
Writing – review & editing: Xiao-Lei Wang, Hejiu Hui, Weiqiang Li

Abstract China's Chang'e-5 (CE-5) mission successfully returned a total of 1.731 kg of lunar material from the north-eastern Oceanus Procellarum region. Young (~2.0 Ga) ages were reported from the CE-5 basalts. However, there are controversies on whether they are low-Ti or high-Ti mare basalt type. Here, we report the results of a comprehensive petrographic, elemental, and Pb isotopic investigation on a 17.6 mg CE-5 basalt clast (CE5C0000YJYX048). By combining high-resolution X-ray tomography of the clast and microbeam (scanning electron microscope SEM, electron probe microanalyzer EPMA) analyses of mineral grains peeled off the clast surface, we derived the bulk clast chemical composition with a very small sample consumption (i.e., <3 mg). The poikilitic clast has a bulk TiO_2 content of 3.78 ± 1.01 wt%, which is representative of a low-Ti basalt end-member in the lunar mare basalts samples. Furthermore, the pyroxene in the studied clast is dominantly pigeonite, in contrast to other reported CE-5 samples where augite is the dominant pyroxene mineralogy. Despite these compositional peculiarities, in situ secondary ion mass spectrometer dating yielded a Pb-Pb age of 2,040 ± 22 Ma for the fragment, which is consistent with ages reported from other CE-5. Based on the chemical and age data analyzed in this study, it can be concluded that the lunar basalts obtained from the CE-5 mission originated from a low-Ti mare basalt-type source. The mineral composition of the mare basalt clast studied, which is dominated by pigeonite, fayalite, and anorthite, likely resulted from late-stage magmatic crystallization when the magma was enriched in Fe.

Plain Language Summary Studying lunar meteorites and samples returned from missions are key ways to conduct scientific research and increase our knowledge of the moon. These methods allow us to move beyond simple observations and make direct measurements of lunar materials. After 45 years from the Apollo and Luna missions, in December 2020, Chang'E-5 (CE-5), China's first lunar mission, returned with a total of 1.731 kg of lunar soil. The basalt clasts in the soil are dated at ~2 billion years ago, which represents the youngest lunar basalt ever studied. The origin of the CE-5 basalts is still debated because it is composed of heterogeneous materials. The CE-5 basaltic clast studied here has a unique mineral composition compared to previous data of other CE-5 basaltic clasts and Apollo basalt samples. This discrepancy is ascribed to the different stages of magma formation in which the occurrence of different minerals subtracted elements and changed the magma's composition. As a result, the heterogeneity of the CE-5 returned lunar basalts relates to different stages of magma evolution. The present project adds new knowledge to understanding the formation of the lunar basalts around the CE-5 landing site.

1. Introduction

The primordial Moon experienced the solidification of early magma ocean and later partial melting of the lunar primordial mantle that produced the mare basalts (Head & Wilson, 2020; Warren, 1985; Zhang et al., 2022). The six Apollo and three Luna missions returned a total of 383 kg of lunar samples, including basalts, which offer direct insights into the chronology and evolution of primordial lunar mare volcanism. Lunar mare basalts are used to reconstruct the thermochemical history of the Moon because the formation of lunar mare basalts is considered to be connected with mantle differentiation (Shearer & Papike, 1999; Wieczorek et al., 2006). Lunar mare basalts display a wider compositional range compared with terrestrial basalts, especially in TiO_2 content (0.3–~15 wt%) (Giguere et al., 2000; Longhi, 1992). For this reason, this oxide is one of the most prominent indicators to classify

the lunar basalts (Giguere et al., 2000; Longhi, 1992; Zhang et al., 2022). Mare basalts returned by the Apollo and Luna missions are traditionally divided into high-Ti (TiO_2 > 6 wt%), low-Ti (TiO_2 1 wt%−6 wt%), and very low-Ti (TiO_2 < 1 wt%) groups (Neal & Taylor, 1992). Using the TiO_2 content to distinguish between various types of mare basalts can be a valuable approach in determining the heterogeneity of the lunar mantle, thermal conditions, and magmatic evolution. The behavior of Ti content in initial crystallizing phases, such as olivine and pyroxene, has the potential to preserve primary characteristics of lunar magma (Johnson, 1998; Zhang et al., 2022).

In December 2020, China's first lunar sample return mission Chang'e-5 (CE-5) successfully brought a total of 1.731 kg of lunar soils to Earth. These soil samples were collected from the north-eastern Oceanus Procellarum at latitude 43.06°N and longitude 51.92°W, about 170 km east-northeast of Mons Rümker (Che et al., 2021; Jiang et al., 2021; Li et al., 2022). While the landing site is situated far from the sampling areas of previous Apollo and Luna missions (Xie et al., 2020), it is located in a region abundant in potassium, rare elements, and phosphorus (KREEP). This area is believed to contain deposits of young mare basalts (Li et al., 2022; Liu et al., 2021). Basaltic clasts from the CE-5 soils have been dated in two ion microprobe Pb-Pb isotope investigations that gave ages of 2,030 ± 4 Ma (Li et al., 2021) and 1,963 ± 57 Ma (Che et al., 2021), respectively. A number of studies have investigated the compositions of the CE-5 mare basalts based on densities, average compositions, and mineral volume abundances (Che et al., 2021; Jiang et al., 2021; Li et al., 2022; Zhang et al., 2022). The reported bulk TiO_2 contents of the CE-5 mare basalts range from 1 to 14.3 wt%, which has led to ongoing debate about the classification of CE-5 basalts in terms of their Ti content (Che et al., 2021; Jiang et al., 2021; Li et al., 2022; Tian et al., 2021; Zhang et al., 2022).

Previous studies on the CE-5 returned basalt samples could reflect the heterogeneity of the samples. If this is the case, it is important to ascertain whether the chemical heterogeneity was caused by mixing between lithological units of the distinct origin or the magmatic evolution of a single source. In particular, if the lunar basalt clasts of different compositions have different ages, then it would be a smoking gun for different rock sources for the basalts at CE-5 landing site. Due to the compositional variability of the CE-5 basalts, additional dating of the returned samples will provide useful constraints for understanding the origin of the CE-5 mare basalts. In this study, a basaltic fragment (CE5C0000YJYX048) from the CE-5 regolith sample collection has been investigated in great detail on petrography, chemical composition, and in situ Pb-Pb isotope geochronology to better understand the petrogenesis and differentiation history of the parental magma of CE-5 mare basalts.

2. Materials and Methods

2.1. Sample Preparation

The CE-5 basaltic clast (#CE5C0000YJYX048) studied in the present work is ∼3 mm in size and 17.6 mg in weight (Figure 1). The clast was placed on a glass slide with a double-sided adhesive tape for microscopic observation and sampling of surface mineral grains (Figures S1, S2a, and S2b in Supporting Information S1). Gentle fingertip force was applied to the clast to roll the clast in all directions when taking microscopic pictures; at the same time, surface mineral grains were peeled off the clast by the adhesive tape (Figures S2a and S2b in Supporting Information S1). By such procedure, more than 150 mineral grains (>1 μm in size) from the clast surface were sampled. The weight loss of the clast before and after such treatment was less than 3 mg. The mineral grains were mounted in two epoxy resin plugs and polished using a diamond slurry (Figures S2c and S2d in Supporting Information S1). Such treatment allowed efficient sampling of ample mineral grains from the clast with minimum sample consumption because all minerals were exposed to the surface of the epoxy resin plug for subsequent scanning electron microscope (SEM) imaging and in situ chemical and isotopic analyses.

2.2. X-Ray Tomography

The 3D distribution of the minerals within the clast was reconstructed by high-resolution X-ray tomographic microscopy (HR-XRTM) using a Zeiss Xradia 520 Versa at the Nanjing Institute of Geology and Paleontology, Chinese Academy of Science (NIGPAS). The instrument was running at 60 kV voltage and 5W power, with a 4X objective and LE5 Filter applied to the scans. Different minerals of X-ray adsorption contrast were distinguished on the tomographic slice (Figure 1b). The tomographic slice images look similar to the backscattered electron (BSE) images and the minerals are characterized by different gray values. A total of 3001 projections (tomographic slice) were taken, with a voxel (pixel) size of 1.7 microns. The HR-XRTM data were processed by ImagJ

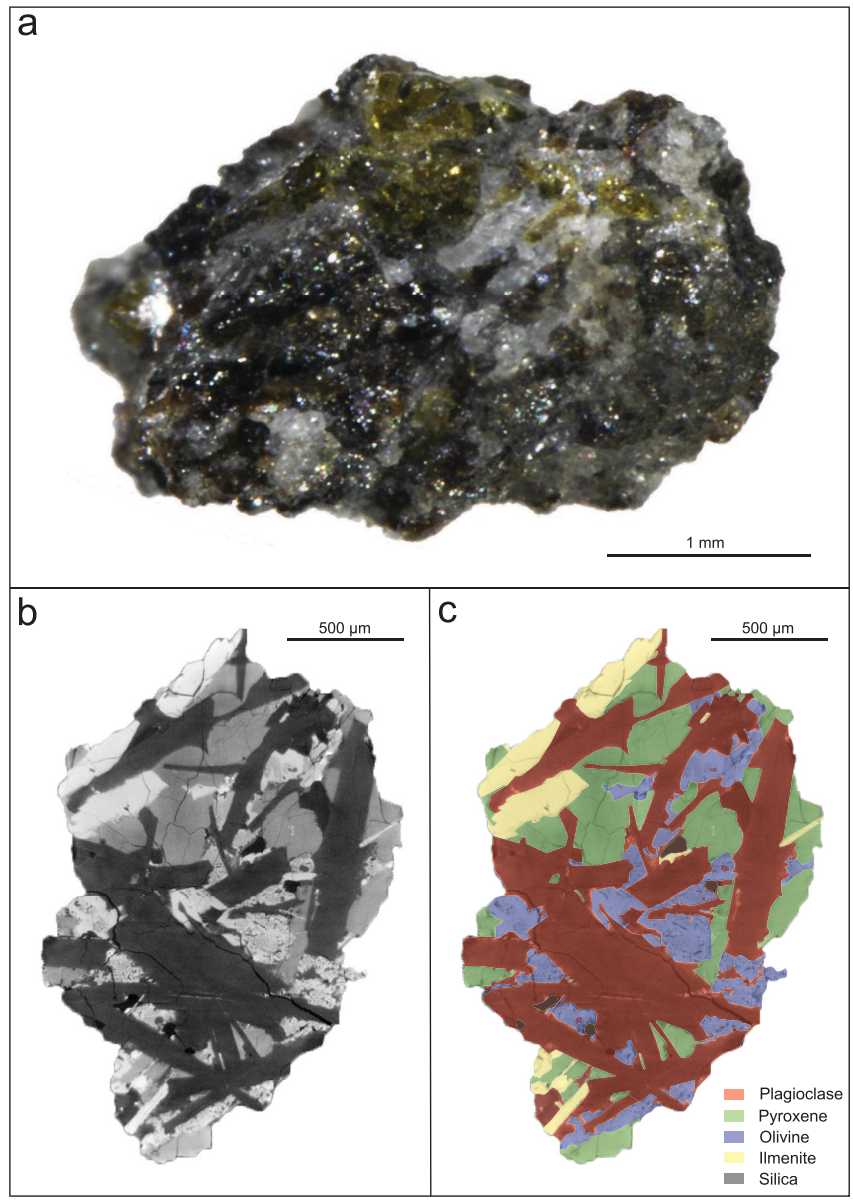

Figure 1. (a) Microscope image of the Chang'e-5 clast CE5C0000YJYX048. (b) X-ray tomographic slice of the Chang'e-5 basalt clast. (c) Colors represent the different groups processed by ImageJ software in order to calculate the modal abundances of major minerals. The groups most likely are composed by different mineral phases.

software to reconstruct the 3D mineralogy of the grain and calculate the modal volume abundance of the mineral phases based on grayscale contrast, with an estimated uncertainty of 2–4 vol%.

2.3. SEM, EPMA, and Calculation of Bulk Chemical Composition

The mineral grains mounted on the two epoxy resin plugs were first imaged with a Hitachi SU-1510 SEM equipped with an Edax EDS at Nanjing University. An acceleration voltage of 15 kV, a beam current ~1 nA, a working distance of 10 mm, and a counting live-time of 80 s were used. Based on back scattered electron imaging and point EDS analysis, a modal distribution of the mineral phases was derived using imageJ software (Figure 1b), and the SEM data were used to correlate the gray values of the HR-XRTM tomographic slice images for different major minerals.

A JEOL JXA-8100 electron probe microanalyzer (EPMA) at Nanjing University was used for analyzing the major element compositions of minerals, with a probe current of 20 nA and acceleration voltage of 15 kV. The

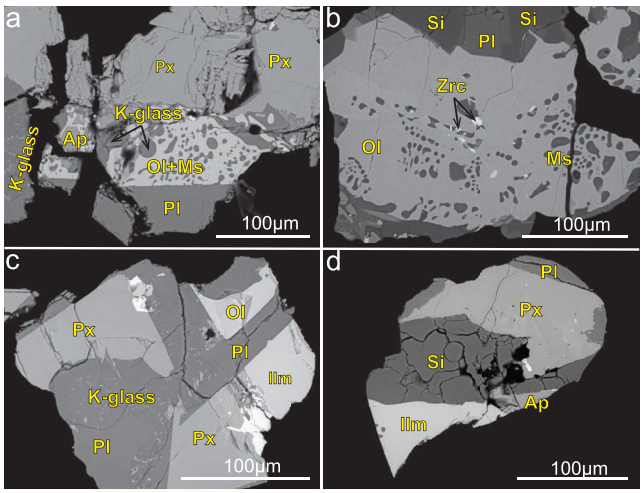

Figure 2. BSE images of the Chang'e-5 sample fragments. Labels indicate different minerals (Px-pyroxene; Pl-Plagioclase; Ilm-ilmenite; Ap-Apatite; Ol-Olivine; Ms-Mesostasis; Zrc-Zirconolite; Si-Silica, and K-glass-potassium rich glass).

elemental results were calibrated using a series of natural minerals and synthetic materials as standards. All EPMA data were reduced with the atomic number-absorption-fluorescence (ZAF) correction procedure.

The bulk composition of the basalt clast was calculated based on the mineral density reported in Treiman et al. (2010), the modal volume abundances of different minerals based on 3D X-ray tomography, and the elemental compositions measured by EPMA for each mineral. The bulk major element compositions were normalized to 100 wt%. Variations in the EPMA data for the minerals were considered and propagated to the uncertainties in bulk chemical composition for the whole clast.

2.4. SIMS Pb-Pb Dating

The in situ lead (Pb) isotopic compositions of the mineral phases were determined using a newly installed CAMECA IMS 1300 HR^3 ion microprobe at Nanjing University. The mounts with candidate minerals were cleaned with a fine (0.5 μm) diamond paste and ethanol to remove the carbon coating before adding a roughly 20-nm gold coating. High-purity oxygen gas was leaked onto the sample surface to enhance the Pb^+ yield in all sessions. Zr-bearing minerals and phosphates, as well as plagioclase, pyroxene, and matrix minerals, were analyzed using a primary O^- beam with spot sizes of approximately 3, 8, and 30 μm, respectively (see Supporting Information S1 for more details). Specifically, the mineral phases analyzed were zirconolite, K-rich glass, apatite, olivine, pyroxene, and ilmenite, and the complete data set is presented in Tables S9–S16 in Supporting Information S1. Because some key mineral phases were small in the sample plugs, the smallest spot size of 2 μm was applied. Pb-Pb isochron was constructed following the methods described in Li et al. (2021) and using the Excel add-in Isoplot (version 4.15).

3. Results

3.1. Petrographic and Textural Characteristics of the CE-5 Lunar Basalt Clast (#CE5C000YJYX048)

The clast has poikilitic texture, in which the mineral grains are relatively coarse (0.1–0.5 mm). The coexisting silicate minerals, including plagioclase, pyroxene, and olivine, display typical intergrowth texture (Figure 2). The main mineral phases include plagioclase (44.7 vol%), pyroxene (37.2 vol%), olivine (7.1 vol%), and ilmenite (6.4 vol%), with small amount of apatite, silica-rich glass, chromite, iron phosphate, and zirconolite phases (total amount 4.6 vol%) (Table 1; Figures 2 and 3). Plagioclase occurs as subhedral laths with lengths of 200–2,000 μm but can also occur either as interstitial grains or intergrowth with pyroxene (Figure 2). Pyroxene occurs as grains up to ~500 μm, with intergrowths of plagioclase (Figure 2). Ilmenite usually occurs as euhedral elongate and blocky crystals (~300 μm in length) (Figure 2). Apatite grains are rare and either enclosed in pyroxene margin or coexist with olivine and mesostasis (Figure 2). The olivine grains are all fayalite and contain K and Si-rich

Table 1
Major Minerals Abundance (vol%) in CE-5 and Apollo Lunar Mare Basalts

Minerals	CE-5[a]	CE-5 YJYX065[b]	CE-5 B1[c]	CE-5 landing site[b]	CE-5 soil[b]	Apollo 11 HT[d]	Apollo 12 LT[d]	Apollo 14 LT[d]	Apollo 15 LT[d]	Apollo 16 HT[d]
Plagioclase	44.7	25.4	34.3	38.7	43.2	35.5	23.2	34.1	24.0	54.0
Pyroxene	37.2	54.4	51.2	44.0	47.7	47.7	68.1	59.2	63.0	40.0
Olivine	7.1	1.3	4.8	8.9	5.4	1.0	3.9	3.2	2.3	5.0
Ilmenite	6.4	17.8	6.7	8.4	3.7	15.0	3.5	2.0	5.7	0.5
Other	4.6	1.0	2.3	0.0	0.0	0.8	1.3.0	1.5	0.0	0.5

[a]Present study. [b]Data from Jiang et al. (2021). [c]Che et al. (2021). [d]Poikilitic basalts fragments from ApolloBasaltB_v2 database (Cone, 2021). (HT) High TiO_2 and (LT) Low TiO_2.

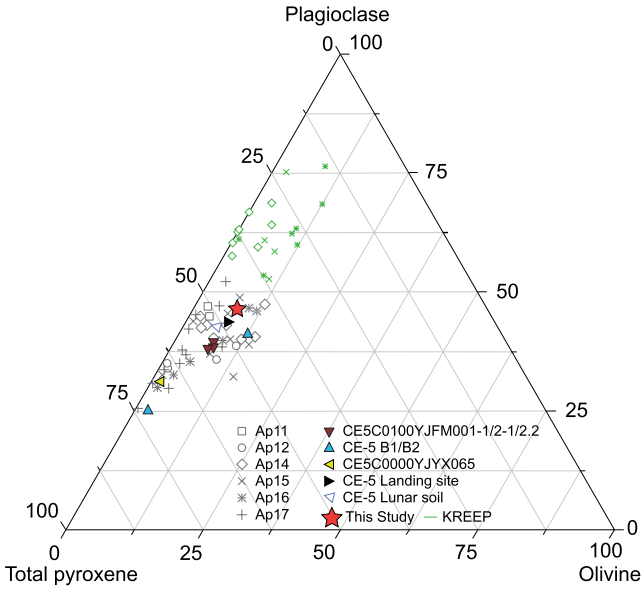

Figure 3. The mineral components of the Chang'e-5 fragment analyzed in this study are compared with those of Apollo, Luna, and previous Chang'e-5 basalt and soil samples. The data for Apollo (Ap) mare basalts fragments and KREEP basalts (marked in green) are sourced from the ApolloBasaltB_v2 database (Cone, 2021),CE5C0100YJFM001-1/2-1/2.2 from Hu et al. (2021), CE-5 B1/B2 from Che et al. (2021), CE5C0000YJYX065 from Jiang et al. (2021), and CE-5 Landing site and Lunar soil are from Liu et al. (2021).

Table 2
Modal Mineralogy of the CE-5 Clast CE5C0000YJYX048

Minerals	Abundance (%)	Total (vol%)
Plagioclase		
Anorthite	98	44.7
Albite	2	
Pyroxene		
Pigeonite	96	37.2
Augite	4	
Olivine		
Fayalite	100	7.1
Forsterite	0	
Ilmenite		6.4
Zr bearing minerals		
Zirconolite	100	0.2
K-rich glass		3.1
Phosphate		
Apatite	100	1.3

Note. The abundance of each mineral was calculated based on the SEM, EPMA, and ImageJ software data.

mesostasis (Figure 2). Additionally, glass composes ~3% of the clast volume and is exclusively associated with mesostasis of fayalite. The glass is free of any textures related to shock metamorphism.

3.2. Mineral Compositions

The feldspar in the studied sample is mainly composed of anorthite (98%) and albite (2%) (Table 2). The anorthite has an average of $An_{85.5}Ab_{13.3}Or_{1.6}$ and the albite has an average of $An_9Ab_{73.5}Or_{12.2}$. These patterns are consistent with previous studies of CE-5 basalts (Jiang et al., 2021; Li et al., 2022). The FeO contents (0.42 wt%−1.57 wt%) of the feldspar are higher than the highland basalt rocks (<0.2 wt%) but analogs to those of Apollo mare basalts (0.25 wt%–1.15 wt%) (Li et al., 2022).

About 96% of the pyroxene are Fe-rich pigeonite with an average composition of $Wo_{26}En_{15}Fs_{60}$ (Table 2). Augite ($Wo_{29}En_{25}Fs_{45}$) is rare (~4%) and orthopyroxene is absent (Figure 4). The pigeonite grains have higher FeO (~25 wt%) and TiO_2 (0.75–2.30 wt%), but lower MgO (2–11 wt%) than those from Apollo 12 (FeO ~ 20 wt%, TiO_2 ~ 0.6 wt%, MgO ~ 14 wt%), 15 (FeO ~ 20 wt%, TiO_2 ~ 0.8 wt%, MgO ~ 16 wt%), and 17 (FeO ~ 18 wt%, TiO_2 ~ 0.7 wt%, MgO ~ 18 wt%) basalt missions samples (Clive Neal's Mare Basalts Database, 2004). Ilmenite contains TiO_2 ~ 50 wt%, MnO ~ 0.4 wt%, and MgO ~ 0.1 wt% which agree with previous CE-5 data. Olivine minerals display only fayalite (Fa) composition (Table 2), with Fo values <15 and low MgO content (0.8 wt%−10 wt%).

3.3. Pb-Pb Isochron Age

In total forty-eight in situ Pb isotope analyses were performed with a CAMECA 1300 HR^3 SIMS on different minerals (including phosphate, potassium-rich glass, plagioclase, pyroxene, olivine, and ilmenite) and two zirconolite grains (Table S9 in Supporting Information S1). The minerals have a large variation in $^{207}Pb/^{206}Pb$ ratios that range between 0.1283 and 0.8495; among them, the zirconolite grains have the most radiogenic signatures (i.e., the lowest $^{204}Pb/^{206}Pb$ and $^{207}Pb/^{206}Pb$ ratios). The in situ Pb isotope data yield a Pb-Pb isochron age of 2,040 ± 22 Ma (Table 5; Figures 5 and 6).

4. Discussion

4.1. Variations in Pyroxene Chemistry for the CE-5 Mare Basalts

The pyroxene chemistry is effective to reconstruct the history of magma crystallization (Alexander et al., 2016). The pyroxene-group minerals commonly follow a crystallization sequence of Ti increasing with Fe and decreasing with Mg (Alexander et al., 2016; Papike et al., 1976). According to the data of this and previous studies, the pyroxene minerals in the CE-5 basalt samples are heterogeneous in chemical composition and contain augite and less orthopyroxene and pigeonite (Che et al., 2021; Li et al., 2021; Tian et al., 2021). Their compositions range from the sub-calcic augite ($Wo_{9.1–41.3}En_{14.6–36.2}Fs_{26.7–72.5}$) to Fe-rich pigeonite ($Wo_{23.8–39}En_{30.2–45.8}Fs_{25.1-80.5}$). The clinopyroxene compositions are plotted together in the pyroxene triangular plot (Figure 4) and they are characterized by a higher Mg content compared to pigeonite. As shown in Figure 7, the clinopyroxene phase mainly formed before the crystallization of ilmenite from the residual magma. The pyroxene chemical compositions

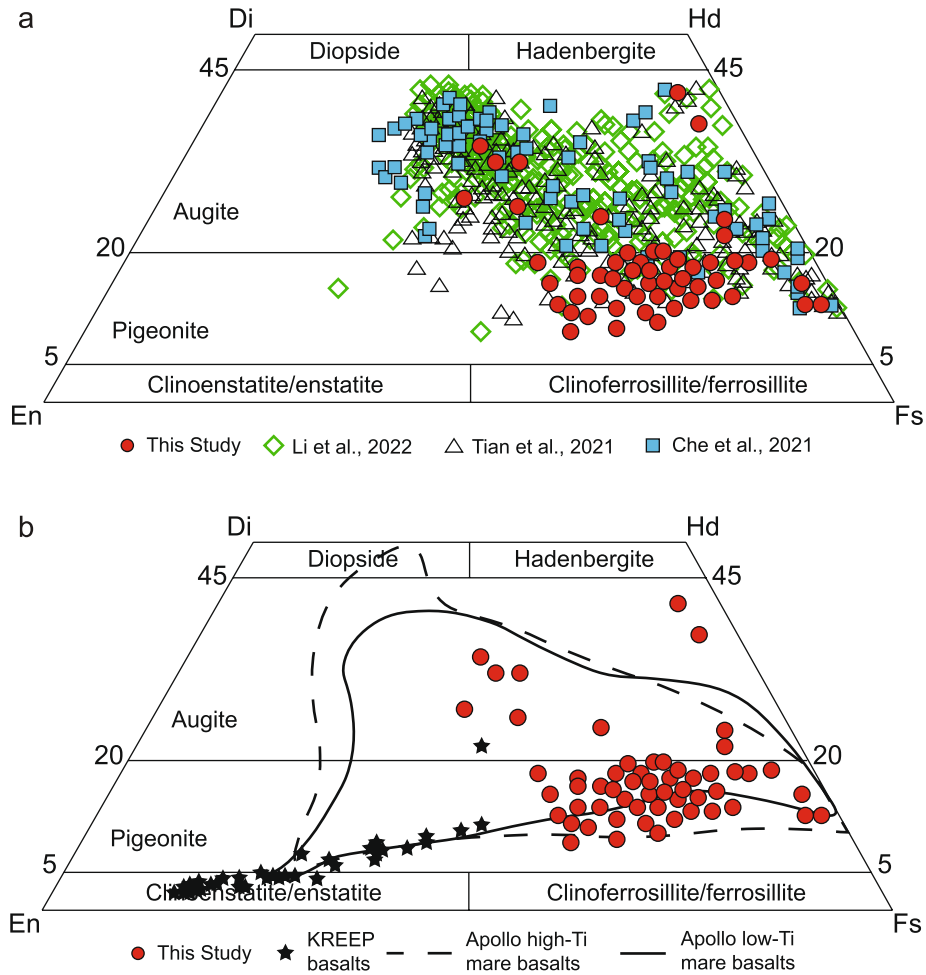

Figure 4. The mineral chemistry of pyroxenes in Chang'e-5 clast CE5C0000YJYX048. (a) The present study data are compared with the previous Chang'e-5 project results. (b) Low-Ti mare basalts from the Apollo 12 and 15 landing sites (MoonDB Search, 2015), high-Ti mare basalts from the Apollo 11 and 17 landing sites (MoonDB Search, 2015), and KREEP basalts composition (MoonDB Search, 2015; Taylor et al., 2012).

exhibit a negative correlation of Mg versus Ti and Fe. The augite is relatively rich in Mg (MgO content between 9 and 20 wt.%; Tian et al., 2021) and crystallized earlier compared to the Fe-rich pigeonite (MgO ~ 4.4 wt%) (Figure 4). In the CE-5 basalt samples, the Ti and Mg contents in olivine grains tend to decrease with the drop of the Fo value (Tian et al., 2021; Zhang et al., 2022). This is consistent with the observation that the olivine contained in clinopyroxene of CE-5 basalt samples are characterized by high Fo (Li et al., 2022; Tian et al., 2021) and confirms that the clinopyroxene and olivine crystallized before the saturation of ilmenite. In this regard, the clinopyroxene in the clast that is mostly composed of Fe-rich pigeonite probably originates from a more evolved melt which became more Fe-rich over time. On the other hand, the late-stage magma is enriched in Fe and it is mainly composed of pyroxene (pigeonite), plagioclase, and less olivine (fayalite). These mineral assemblages display intergrowth textures and they most likely cocrystallized in the sample almost simultaneously (Alexander et al., 2016).

4.2. Bulk Chemical Composition of CE-5 Mare Basalts: High Ti- or Low Ti- Type?

In this study, we applied a low-sample consumption method to derive the bulk chemical composition of the lunar basalt clast sample by combining 3D X-ray tomography and in situ analyses. The results show that the studied lunar basalt clast is characterized by higher iron (FeO 23.32 ± 2.06 wt%), titanium (TiO_2 3.78 ± 1.01 wt%), and lower aluminum (Al_2O_3 11.95 ± 1.55 wt%) than the most Luna and Apollo low-Ti basalt samples (Table 4; Figure 8).

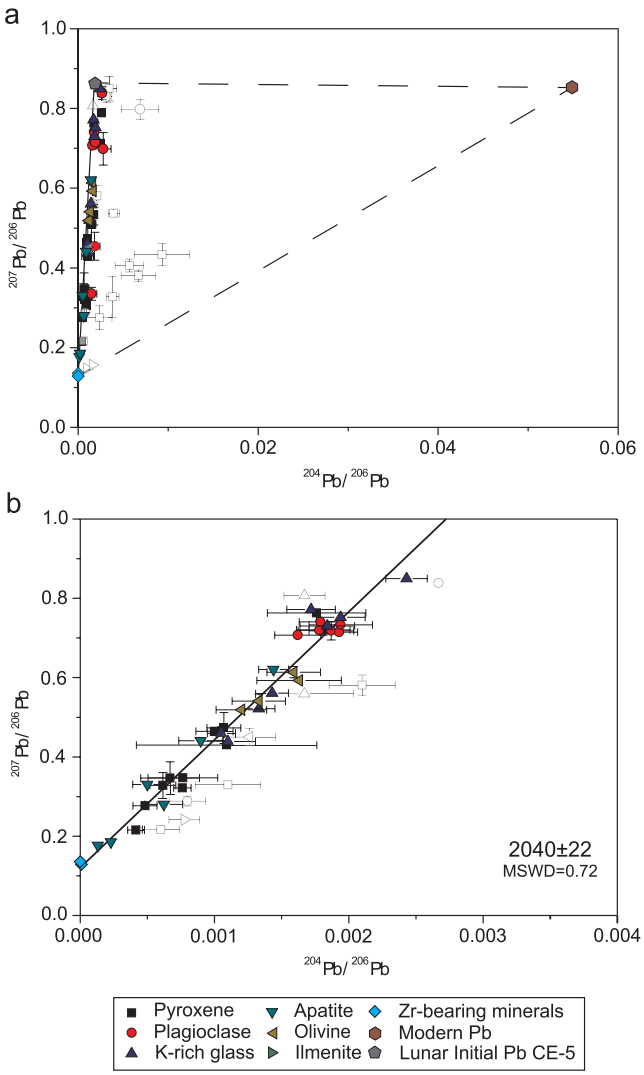

Figure 5. Chang'e-5 basalts clast Pb-Pb isochrons. (a) Data from all the minerals analyzed. The isochrons calculation was based only on the spots very close to the lunar initial-radiogenic Pb mixing line. The spots not on that line were affected by terrestrial contamination. The triangle areas represent the mixing trend among the initial Pb component, the radiogenic Pb, and the current terrestrial Pb composition. (b) Lowest portion of the isochron showing the data with low $^{204}Pb/^{206}Pb$. Error bars represent 1σ standard error. The data points not included in the isochron calculation are marked by low opacity and open symbols.

Alternatively, the TiO_2 content of the basaltic magma can be estimated from the chemical compositions of the earliest formed magnesian pyroxene and the partition coefficient of Ti between pyroxene and basaltic magma following the $D(TiO_2)_{(px/basalt)}$ of Robinson et al. (2012). Using the following equation: $D\ TiO_{2\ (px/basalt)} = [0.0148 \times (CaO_{px}) + 0.09] \pm 0.05\ (2\sigma)$, the calculated bulk rock TiO_2 content varies between 2.9 wt% and 5.1 wt% with an average of 3.66 ± 1.55 wt%.

Therefore, the average bulk TiO_2 content for the studied basaltic clast estimated by the two different approaches converges at around 3.66 ± 1.53–3.78 ± 1.01 wt%, well within the low-Ti field of mare basalts (1–6 wt%; Neal & Taylor, 1992) (Tables 3 and 4; Figures 7 and 8). As shown in Figure 8, the sample plots in the same area of the Apollo 14, 15, and 16 basalts. In Figure 4 the mineral composition of the clast is close to Apollo 14 and 15 basalts, supporting a low-Ti basalt origin. Based on the results, the investigated CE-5 basalt clast belongs to a low TiO_2 (3.5–5.7 wt%) and high FeO (22.2–23.5 wt%) mare basalt source.

The origin of the CE-5 basalt source is still a topic of debate. Some studies suggest a low-Ti type (Li et al., 2022; Tian et al., 2021; Zhang et al., 2022), while others propose a high-Ti type (Che et al., 2021; Jiang et al., 2021) for the bulk rock compositions. The inconsistency in the results may be attributed to the small sample sizes and the fact that most of the published data are close to the statistical boundary between high-Ti and low-Ti mare basalts (Figure 8). Additionally, the heterogeneous composition of the CE-5 basalts might have contributed to the conflicting findings. According to He et al. (2022), most of the previous CE-5 samples can be considered low-intermediate Ti, rather than high-Ti. Out of all the fragments analyzed, only the one studied by Jiang et al. (2021) exhibits a clear high-Ti composition, as reported by He et al. (2022) and Zhang et al. (2022). As a result in this paper, it is probable that the lunar soil from the CE-5 mission originates from a source with low TiO_2 content, with a potential minor contribution from volcanic and impact materials to account for the high-Ti data reported by Jiang et al. (2021), as noted by He et al. (2022).

4.3. Age of the Lunar Basalts at the Chang'e-5 Landing Site

A common process on the lunar surface is the mixing of local and distant ejecta materials, as well as meteoritic fragments. Ejecta or exotic materials can be provided by impact mixing processes that usually imply movement from a lower stratigraphic level to a higher level and thus the clasts sampled on the Moon's surface can be composed of different types of materials (Korotev et al., 2011; Korotev & Gillis, 2001). This process has been observed in most of the Apollo samples (McKenzie & O'nions, 1991) as well as the CE-5 samples (Zong et al., 2022). Remote sensing studies of the CE-5 landing site estimated the contribution of exotic, nonmare material from <10% to up to 40% (Liu et al., 2021; Qian et al., 2021). The results from Zong et al. (2022) showed that exotic additions of the highland and KREEP materials in the CE-5 soil are less than 3% and 5%, respectively. Sheng et al. (2022) also estimated a highland component of CE-5 soil at ~3%. Mixing of ejecta and meteoritic materials could have significant consequences on the geochronology of the CE-5 basalts, not only because such a process might have introduced materials of different ages but also because such a process can be associated with impact events that reset the U-Pb isotope systems in the CE-5 basalts. The lunar basalt sample investigated in this study, however, only displays pristine texture without any sign of overprinting from shock metamorphism. Based on these textural observations, it can be inferred that the studied clast is not a result of mixing of external materials or shock impacts.

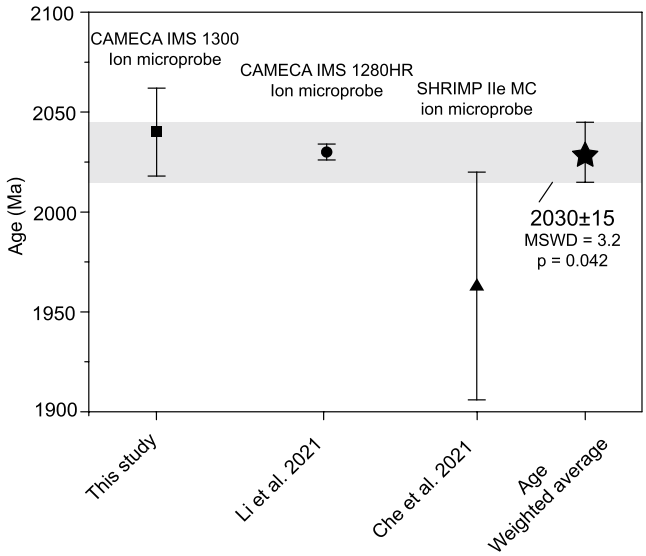

Figure 6. Comparison of Chang'e-5 basalts clast Pb-Pb ages from different studies.

To estimate the age of the CE-5 sample under study, different mineral phases were employed (refer to the results section). Generally, glass is more susceptible to resetting by shock events, which leads to exchange of Pb, and therefore should not be included in the estimation. Conversely, Zr-rich minerals are more likely to maintain their original Pb-isotope compositions even when subjected to shock (Che et al., 2021; Moser et al., 2013). In the present project, the estimated age did not exhibit a significant decrease of $^{207}Pb/^{206}Pb$ common in shocked-induced material (see Figure 5). Nonetheless, we highlight that the sample itself does not exhibit any textural sign of shock metamorphism. The Pb-Pb isochron age of 2,040 ± 22 Ma (Table 5; Figure 5) obtained in this study overlaps with the Pb-Pb age of both Che et al. (2021) (1,963 ± 57 Ma) and Li et al. (2021) (2,030 ± 4 Ma), given the error bars of 95%-level of confidence (Figure 6). This chronological overlapping between the three ages rules out the possibility that the basalt clast analyzed in this study had a fundamentally different magmatic origin or source than the other CE-5 lunar basalts that had been reported in other studies, even the lunar basalt clast in this study contains different pyroxenes (pigeonite) than the other CE-5 samples. Assuming that all the three in situ Pb-Pb ages correspond to a single lunar basaltic magma eruption event, then the age of that putative single magmatic event could be estimated by taking the error-weighted average of the three in situ Pb-Pb ages, which is 2,030 ± 15 Ma (Figure 6). However, it should be noted that CE-5 basaltic magmas may have experienced multiple eruption processes or complicated magmatic evolution processes, which generated different types of basaltic rocks as observed so far. For example, it has been proposed that a minor contribution from high-Ti volcanism (Jiang et al., 2021) might be transported to the CE-5 landing site through volcanic processes. If it is the case, additional high-precision dating on more CE-5 samples will be needed to fully resolve the fine magmatic history of the basaltic magmatism from a geochronological perspective in the future.

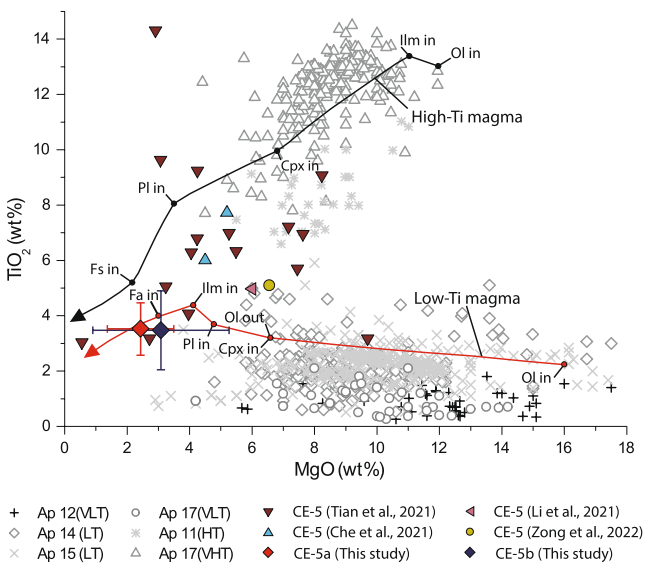

Figure 7. MgO versus TiO_2 (wt%) in Chang'e-5 and Apollo mare basalts. The present study data marked as CE-5a represent the bulk calculation using the vol% of the different mineral phases from ImagJ software and the CE-5b following Tian et al. (2021) approach. Apollo data are form the ApolloBasaltB_v2 database (Cone, 2021). The labels represent the different mare basalts types based on the titanium content (VLT-very low titanium, LT-low titanium, HT-high titanium, and VHT-very high titanium). The broken lines represent the fractional crystallization of the high-Ti, black line, and low-Ti magma, red line. Modified from Zhang et al. (2022).

4.4. Implications for Petrogenesis of Chang'e-5 Basalt

The CE-5 basaltic clasts can be texturally subdivided into five types mainly based on the mineral grain size: aphanitic (typically <0.01 mm), porphyritic (typically <0.05 mm and phenocrysts with grain sizes up to 0.5 mm), ophitic/subophitic (<0.1 mm), poikilitic (0.1–0.5 mm) and equigranular (0.1–0.5 mm). The basaltic clast investigated in this study has a poikilitic texture. The composition of the clast CE5C0000YJYX048 is substantially different from previously studied CE-5 basaltic clasts. The total plagioclase content of the present sample is 44.7 vol%, significantly higher than the average of the previously reported CE-5 fragments (~35 vol%) and Apollo 11 and 14 basalts (~23 vol%) but within the range of Apollo 16 and Apollo 15 pigeonite (28.1 vol%–64.3 vol%, respectively) (Table 1; Figure 3). Pyroxene content (37.2 vol%) of this study is lower than those of the previously reported CE-5 basalts sample from Che et al. (2021) (~51 vol%) and Apollo 11, 12, 14, 15, 16 basalts fragments (47 vol%, 68.1 vol%, 59.2 vol%, 63 vol%, and 40 vol%, respectively) (Table 1; Figure 3) (Cone, 2021). The olivine content is 7%, close to other CE-5 and Apollo basalts samples (Table 1; Figure 3). The glass composes only ~3% of the clast which is considerably lower than those of the Apollo missions (~25 vol%) (Cone, 2021). The glass observed in the sample was formed during the final stage of lunar basaltic magma crystallization. Notably, this glass is free of any textures related to shock metamorphism, suggesting that it formed in situ.

During the reconstruction of the petrology and the bulk composition of the lunar basalt samples, the issue of representativeness of the small amount of the studied material needs to be carefully considered. This could lead to

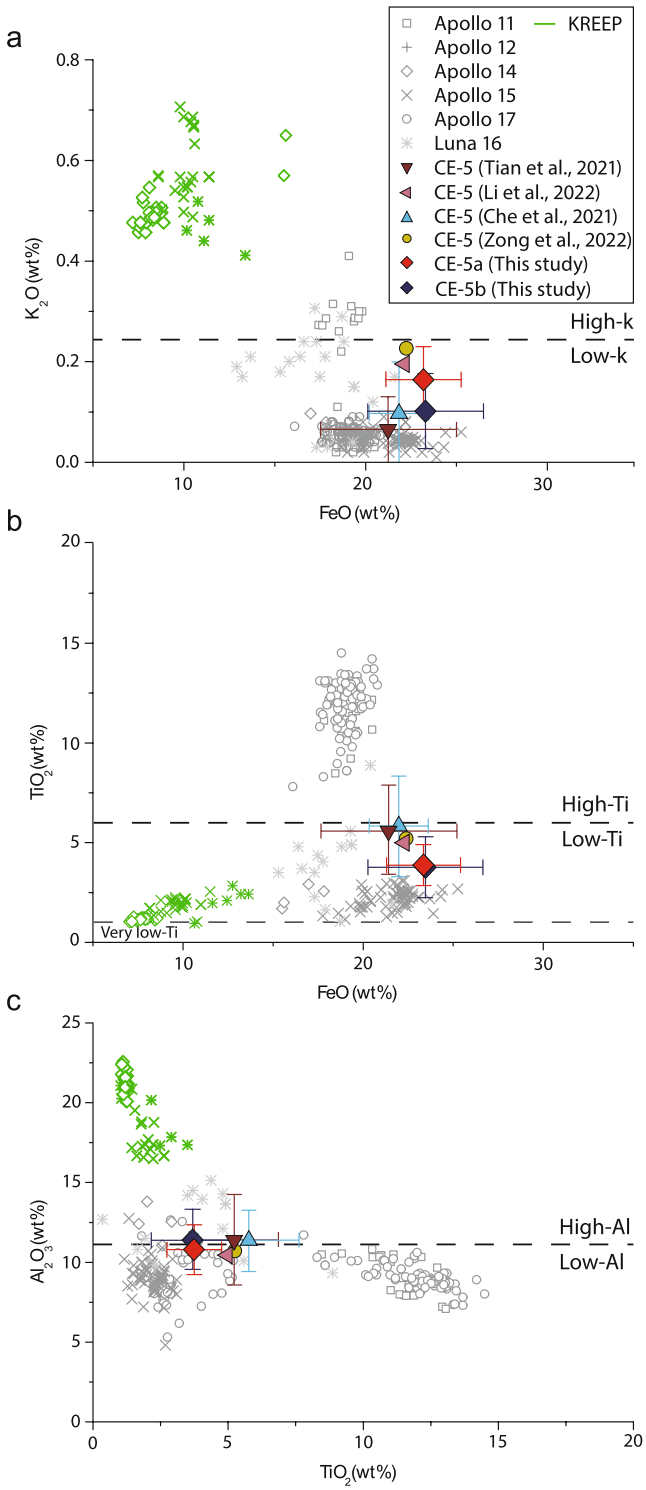

Figure 8. Chang'e-5 mare basalts diagrams of the estimated bulk composition. CE-5a contains the results from the bulk composition calculated by using the vol% of minerals from ImagJ software and CE-5b following Tian et al. (2021) approach. The Apollo and Luna mare basalts fragments data are from Clive Neal's Mare Basalts Database (2004) (https://www3.nd.edu/~cneal/Lunar-L/). The Apollo KREEP basalts data are marked in green.

errors and overinterpretation of samples that may be too small to be representative of the parent lava flows (Neal & Taylor, 1992; Snape et al., 2014). In order to estimate the bulk composition, different approaches were applied such as estimating the modal mineralogy following Tian et al. (2021) and Jiang et al. (2021) and using the estimated vol% of the minerals phases. The results from these methods were also compared to those from previous studies (Table 3).

The prolonged volcanism observed at the CE-5 landing site remains unclear, but it has been suggested that it was not caused by radiogenic heating (Che et al., 2021; Li et al., 2021; Tian et al., 2021) or hydrous melting (Hu et al., 2021; Wang et al., 2015). The CE-5 basalts are evolved and enriched in mafic minerals (Sheng et al., 2022). Lunar mare basalts are characterized by decreasing in Mg content in bulk rock composition, from the early stage magma that was rich in Mg to the last stage magmas that was mostly enriched in Fe (Zhang et al., 2022). For example, in olivine and pyroxene, the Mg value decreased from the earlier stage in which mainly crystallized forsterite, augite, and clinopyroxene to the late stages mostly composed by Fe-rich fayalite with mesostasis and pigeonite (Jiang et al., 2021; Ji et al., 2022; Zhang et al., 2022; Wang et al., 2015). The major phases presented in the clast are anorthite (plagioclase), pigeonite (pyroxene), fayalite (olivine), and ilmenite. This mineral assemblage corresponds to the late stage of the basalt fractionation process (Table 2; Figures 4–6). Additionally, these minerals display strong intergrowth that are indicative of simultaneous crystallization (Figure 2). This process might explain the higher plagioclase content of the clast compared with previous CE-5 mare basalts fragments in which the commonly euhedral plagioclase laths are filled with pyroxene and olivine grains (Li et al., 2022). The extended process of magma fractionation, as observed in this study, likely played a significant role in contributing to the compositional variability observed at the CE-5 landing site. Therefore, the mineral composition of the studied mare basalt clast, dominated by pigeonite, fayalite, and anorthite, is likely indicative of the specific stage of crystallization at which these clasts were formed.

5. Conclusions

In this study, we developed a low-sample-consumption method (<3 mg) to characterize the mineralogical and elemental composition of lunar rock samples. We applied this method to a mare basalt clast (#CE5C0000YJYX048) returned from China's Chang'e-5 mission. This sample, due to its small size (17.6 mg), is unlikely to fully represent its parental melts in terms of bulk chemistry and modal mineralogy. However, this limitation might be overcome by combining different analytical results such as bulk chemical estimations, major elements and components of individual minerals, from different CE-5 samples, including the clast studied in this study and those reported in literature. Hence, it is still possible to study the petrogenesis and differentiation history of the basaltic magmas at the CE-5 landing site.

The basalt clast (#CE5C0000YJYX048) shows unusual mineralogical compositions, different from previous data of CE-5 basalts. It contains higher iron (FeO 23.32 ± 2.06 wt%), titanium (TiO_2 3.78 ± 1.01 wt%), and lower aluminum (Al_2O_3 11.95 ± 1.55 wt%) compared with the Luna and Apollo low-Ti basalts and clearly belongs to low-Ti/low-Al and low-K mare basalt type. We also report a new high-precision in situ Pb-Pb age of 2,040 ± 22 Ma from the CE-5 basalt clast. This age overlaps with the two

Table 3
Bulk Chemical Composition of CE-5 Clast CE5C0000YJYX048

Major element												
Element (wt%)	SiO_2	TiO_2	Al_2O_3	Cr_2O_3	FeO	MnO	MgO	CaO	Na_2O	K_2O	P_2O_5	Total
CE-5a[a]	44.49	3.78	10.95	0.03	23.32	0.26	2.47	13.32	0.68	0.16	0.54	100
±SD	3.76	1.01	1.55	0.01	2.06	0.09	1.06	2.07	0.35	0.06	0.01	–
CE-5b[b]	43.10	3.73	11.59	0.04	23.47	0.30	3.12	13.42	0.85	0.10	0.28	100
±SD	3.85	1.53	1.86	0.02	3.18	0.10	2.17	2.29	0.07	0.07	0.03	–

[a]Major element estimated using mineral phases vol%. [b]Major element estimated following the approach described in Tian et al. (2021).

Table 4
Bulk Chemical Composition (wt%) of CE-5 and Apollo Lunar Basalts

	SiO_2	TiO_2	Al_2O_3	Cr_2O_3	FeO	MnO	MgO	CaO	Na_2O	K_2O	P_2O_5	Total
CE-5[a]	44.49	3.78	10.95	0.03	23.32	0.26	2.47	13.32	0.68	0.16	0.54	100.0
CE-5[b]	42.20	5.00	10.80	–	22.50	0.28	6.48	11.00	0.26	0.19	0.23	98.94
CE-5-B1[c]	41.75	5.70	11.60	0.14	22.20	0.29	4.49	11.64	0.34	0.10	0.21	98.05
CE-5[d]	41.25	5.12	11.50	0.00	22.70	0.28	6.52	11.64	0.46	0.21	0.27	99.90
Apollo 12 Ol	49.40	1.29	0.90	0.13	25.70	0.44	11.10	10.50	–	–	–	99.46
Apollo 12 Pig	53.51	0.35	0.66	0.74	16.69	0.29	24.26	2.61	–	–	–	99.23
Apollo 14	51.30	0.84	1.73	0.73	18.60	–	21.20	4.37	0.02	–	–	98.79
Apollo 15 Ol	49.90	1.21	1.66	0.22	25..80	–	11.40	10.60	–	–	–	100.7
Apollo 15 Pg	52.40	0.36	1.89	1.04	16.90	–	23.90	2.62	0.03	–	–	99.14
Apollo 14 KREEP	52.40	0.36	1.89	1.04	16.90	–	23.90	2.62	0.03	–	–	99.14

[a]Present study. [b]Data from Li et al. (2022). [c]Che et al. (2021). [d]Zong et al. (2022). Apollo missions date are from ApolloBasaltB_v2 database (Cone, 2021). The terms Ol (olivine) and Pg (pigeonite) are used to describe different basal chemical types of basalts. For example, olivine basalts are relatively high in either Mg or Fe, while pigeonite basalts are relatively Si-rich (Papike et al., 1976).

Table 5
Summary of Chemical Compositions and Age of the Apollo Low-Ti and CE-5 Mare Basalts

Name	CE-5[a]	CE-5[b]	CE-5[c]	Apollo 12 Pig	Apollo 12 Ol	Apollo15 Pig	Apollo 15 KREEP
Age (Ga)	2.04	2.03	~2.00	~3.13–3.18	~3.15–3.17	~3.15–3.17	3.89
FeO (wt%)	23.5	22.2	22.7	21.0	20.6	21.3	10.0
TiO_2 (wt%)	3.73	5.7	5.14	3.00	3.60	2.10	2.00
Al_2O_3 (wt%)	10.6	11.6	11.5	8.01	9.20	8.90	15.5
K_2O (wt%)	0.10	0.19	0.21	0.06	0.07	0.04	0.60
$Mg^{\#}$	33.3	32.1	46.8	52.1	46.6	44.8	61.1
Th (ppm)	0.82	4.5	5.14	1.09	0.74	0.56	11.5
La (ppm)	23.6	37.5	35.4	6.6	5.8	5.40	72.0

[a]Present study. [b]Data from Tian et al. (2021). [c]Zong et al. (2022). Age data of Apollo low-Ti basalts are from Snape et al. (2019); Apollo basalts elements data are from ApolloBasaltB_v2 database (Cone, 2021) and Wieczorek et al. (2006).

published in situ Pb-Pb ages within analytical uncertainty. Therefore, it rules out the possibility that the basaltic clast analyzed in this study had a fundamentally different magmatic origin or source than the CE-5 lunar basalts reported in other studies. The error-weighted average of the three in situ Pb-Pb ages is 2,030 ± 15 Ma. We propose that the variation in mineral phases (specifically, pigeonite, fayalite, and anorthite) and bulk rock compositions in other CE-5 basalts data are likely the result of late-stage magmatic crystallization, leading to compositional diversity.

Data Availability Statement

The data used for interpreting the crack growth and microflake formation in this study are provided as tables and Supporting Information S1 in this paper. The results from the present paper were combined with databases from different sources: (a) The previous reported CE-5 minerals assemblages and soil elemental bulk compositions are available in Che et al. (2021), Li et al. (2021), Jiang et al. (2021), Tian et al. (2021), Zhang et al. (2022), and Zong et al. (2022) (and their supplementary files information). (b) The CE-5 Pb-Pb estimated ages are from Che et al. (2021) and Li et al. (2021). (c) Apollo and Luna datasets are from Papike et al. (1982), Neal and Taylor (1992), Snape et al. (2019), Wieczorek et al. (2006), Taylor et al. (2012), and Cone (2021). (d) Apollo data missions are accessible at MoonDB Search (2015) (http://search.moondb.org/) and Clive Neal's Mare Basalts Database (2004) (https://www3.nd.edu/~cneal/Lunar-L/). The CE-5 mare basalt evolution model is reported by Wang et al. (2015), Alexander et al. (2016), and Zhang et al. (2022). The software ImageJ, accessible at https://imagej.nih.gov/ij/, was mainly used to derive the modal distribution of the mineral phases in the clast.

Acknowledgments
This work was supported by the National Natural Science Foundation of China (No. 42241120 W.L. and No. 42241121 to XL.W.), China National Space Administration (CNSA) Grant (D020205 to H.H.), and the State Key Laboratory for Mineral Deposits Research and the Fundamental Research Funds for the Central Universities (Grant 0206-14380179). We are grateful to the China National Space Administration for providing the Chang'E-5 basalt fragment. We thank Yang He for the EPMA analyses support, Xie Wenli for making the epoxy resin plugs, and Bidong Zhang and one anonymous reviewer for their constructive comments.

References

Alexander, L., Snape, J. F., Joy, K. H., Downes, H., & Crawford, I. A. (2016). An analysis of Apollo lunar soil samples 12070,889, 12030,187, and 12070,891: Basaltic diversity at the Apollo 12 landing site and implications for classification of small-sized lunar samples. *Meteoritics & Planetary Sciences*, *51*(9), 1654–1677. https://doi.org/10.1111/maps.12689

Che, X., Nemchin, A., Liu, D., Long, T., Wang, C., Norman, M. D., et al. (2021). Age and composition of young basalts on the moon, measured from samples returned by Chang'E-5. *Science*, *374*(6569), 887–890. https://doi.org/10.1126/science.abl7957

Clive Neal's Mare Basalts Database. (2004). Retrieved from https://www3.nd.edu/~cneal/Lunar-L/

Cone, K. A. (2021). ApolloBasalt DB_V2, version 1.0. *Interdisciplinary Earth Data Alliance (IEDA)*. https://doi.org/10.26022/IEDA/111982

Giguere, T. A., Taylor, G. J., Hawke, B. R., & Lucey, P. G. (2000). The titanium contents of lunar mare basalts. *Meteoritics & Planetary Sciences*, *35*(35), 193–200. https://doi.org/10.1111/j.1945-5100.2000.tb01985.x

He, Q., Li, Y., Baziotis, I., Qian, Y., Xiao, L., Wang, Z., et al. (2022). Detailed petrogenesis of the unsampled Oceanus Procellarum: The case of the Chang'e-5 mare basalts. *Icarus*, *383*, 115082. https://doi.org/10.1016/j.icarus.2022.115082

Head, J. W., & Wilson, L. (2020). Rethinking lunar mare basalt regolith formation: New concepts of lava flow protolith and evolution of regolith thickness and inter-nal structure. *Geophysical Research Letters*, *47*(20), e2020GL088334. https://doi.org/10.1029/2020GL088334

Hu, S., He, H., Ji, J., Lin, Y., Hui, H., Anand, M., et al. (2021). A dry lunar mantle reservoir for young mare basalts of Chang'E-5. *Nature*, *600*(7887), 49–53. https://doi.org/10.1038/s41586-021-04107-9

Ji, J., He, H., Hu, S., Lin, Y., Hui, H., Hao, J., et al. (2022). Magmatic chlorine isotope fractionation recorded in apatite from Chang'e-5 basalts. *Earth and Planetary Science Letters*, *591*(591), 117636. https://doi.org/10.1016/j.epsl.2022.117636

Jiang, Y., Li, Y., Liao, S. Y., Yin, Z. J., & Hsu, W. B. (2021). Mineral chemistry and 3D tomography of a chang'E 5 high-Ti basalt: Implication for the lunar thermal evolution history. *Science Bulletin*, *67*(7), 755–761. https://doi.org/10.1016/j.scib.2021.12.006

Johnson, K. T. (1998). Experimental determination of partition coefficients for rare Earth and high-field-strength elements between clinopyroxene, garnet, and basaltic melt at high pressures. *Contributions to Mineralogy and Petrology*, *133*(133), 60–68. https://doi.org/10.1007/s004100050437

Korotev, R. L., & Gillis, J. J. (2001). A new look at the Apollo 11 regolith and KREEP. *Journal of Geophysical Research*, *106*(E6), 12339–12353. https://doi.org/10.1029/2000JE001336

Korotev, R. L., Jolliff, B. L., Zeigler, R. A., Seddio, S. M., & Haskin, L. A. (2011). Apollo 12 revisited. *Geochimica et Cosmochimica Acta*, *75*(75), 1540–1573. https://doi.org/10.1016/j.gca.2010.12.018

Li, C. L., Hu, H., Yang, M., Pei, Z., Zhou, Q., Ren, X., et al. (2022). Characteristics of the lunar samples returned by Chang'E-5 mission. *National Science Review*, (9), nwab188. https://doi.org/10.1093/nsr/nwab188

Li, Q. L., Zhou, Q., Liu, Y., Xiao, Z., Lin, Y., Li, J., et al. (2021). Two billion-year-old volcanisms on the Moon from Chang'E-5 basalts. *Nature*, *600*(7887), 54–58. https://doi.org/10.1038/s41586-021-04100-2

Liu, J., Zeng, X., Li, C., Ren, X., Yan, W., Tan, X., et al. (2021). Landing site selection and overview of China's lunar landing missions. *Space Science Reviews*, *217*(1), 6. https://doi.org/10.1007/s11214-020-00781-9

Longhi, J. (1992). Experimental petrology and petrogenesis of mare volcanics. *Geochimica et Cosmochimica Acta*, *56*(56), 2235–2251. https://doi.org/10.1016/0016-7037(92)90186-M

McKenzie, D., & O'nions, R. (1991). Partial melt distributions from inversion of rare Earth element concentrations. *Journal of Petrology*, *32*(32), 1021–1091. https://doi.org/10.1093/petrology/32.5.1021

MoonDB Search. (2015). Retrieved from http://search.moondb.org/

Moser, D. E., Chamberlain, K. R., Tait, K. T., Schmitt, A. K., Darling, J. R., Barker, I. R., & Hyde, B. C. (2013). Solving the Martian meteorite age conundrum using micro-baddeleyite and launch-generated zircon. *Nature*, *499*(7459), 454–457. https://doi.org/10.1038/nature12341

Neal, C. R., & Taylor, L. A. (1992). Petrogenesis of mare basalts: A record of lunar volcanism. *Geochimica et Cosmochimica Acta*, *56*(56), 2177–2211. https://doi.org/10.1016/0016-7037(92)90184-K

Papike, J. J., Hodges, F. N., Benc, A. E., Cameron, M., & Rhodes, J. M. (1976). Mare basalts: Crystal chemistry, mineralogy and petrology. *Reviews of Geophysics and Space Physics*, *14*(14), 475–540. https://doi.org/10.1029/RG014i004p00475

Papike, J. J., Simon, S. B., & Laul, J. C. (1982). The lunar regolith: Chemistry, mineralogy, and petrology. *Reviews of Geophysics and Space Physics*, *20*(20), 761–826. https://doi.org/10.1029/RG020i004p00761

Qian, Y., Xiao, L., Head, J. W., van der Borget, C. H., Hiesinger, H., & Wilson, L. (2021). Young lunar mare basalts in the Chang'E-5 sample return region, northern Oceanus procellarum. *Earth and Planetary Science Letters*, *555*(555), 116702. https://doi.org/10.1016/j.epsl.2020.116702

Robinson, K. L., Treiman, A. H., & Joy, K. H. (2012). Basaltic fragments in lunar feldspathic meteorites: Connecting sample analyses to orbital remote sensing. *Meteoritics & Planetary Sciences*, *47*(47), 387–399. https://doi.org/10.1111/j.1945-5100.2012.01344.x

Shearer, C., & Papike, J. (1999). Magmatic evolution of the Moon. *American Mineralogist*, *84*(84), 1469–1494. https://doi.org/10.2138/am-1999-1001

Sheng, S. Z., Chen, Y., Zhang, B., Hao, J. H., & Wang, S. J. (2022). First location and characterization of lunar highland Tas in Chang'E-5 Breccias using TIMA-SEM-EPMA. *Atomic Spectroscopy*, (43), 352–363. https://doi.org/10.46770/AS.2022.030

Snape, J. F., Jo, K. H., Crawford, I. A., & Alexander, L. (2014). Basaltic diversity at the Apollo 12 site: Inferences from petrologic examinations of the soil sample 12003. *Meteoritics & Planetary Sciences*, *49*(5), 842–871. https://doi.org/10.1111/maps.12285

Snape, J. F., Nemchin, A. A., Whitehouse, M. J., Merle, R. E., Hopkinson, T., & Anand, M. (2019). The timing of basaltic magmatism at the Apollo landing sites. *Geochimica et Cosmochimica Acta*, *266*(266), 29–53. https://doi.org/10.1016/j.gca.2019.07.042

Taylor, G. J., Martel, L. M. V., & Spudis, P. D. (2012). The Hadley-Apennine KREEP basalt igneous province. *Meteoritics & Planetary Sciences*, *47*(5), 861–879. https://doi.org/10.1111/j.1945-5100.2012.01364.x

Tian, H. C., Wang, H., Chen, Y., Yang, W., Zhou, Q., Zhang, C., et al. (2021). Non-KREEP origin for Chang'E-5 basalts in the procellarum KREEP Terrane. *Nature*, *600*(7887), 59–63. https://doi.org/10.1038/s41586-021-04119-5

Treiman, A. H., Maloy, A. K., Shearer, C. K., & Gross, J. (2010). Magnesian anorthositic granulites in lunar meteorites Allan Hills A81005 and Dhofar 309: Geochemistry and global significance. *Meteoritics & Planetary Sciences*, *45*(45), 163–180. https://doi.org/10.1111/j.1945-5100.2010.01014.x

Wang, K., Jacobsen, S. B., Sedaghatpour, F., Chen, H., & Korotev, R. L. (2015). The earliest lunar magma ocean differentiation recorded in Fe isotopes. *Earth and Planetary Science Letters*, *430*(430), 202–208. https://doi.org/10.1016/j.epsl.2015.08.019

Warren, P. H. (1985). The magma ocean concept and lunar evolution. *Annual Review of Earth and Planetary Sciences*, *13*(1), 201–240. https://doi.org/10.1146/annurev.ea.13.050185.001221

Wieczorek, M. A., Jolliff, B. L., Khan, A., Pritchard, E., Weiss, B. P., Williams, J. G., et al. (2006). The constitution and structure of the lunar interior. *Reviews in Mineralogy and Geochemistry*, *60*(60), 221–364. https://doi.org/10.2138/rmg.2006.60.3

Xie, M., Xiao, Z., Zhang, X., & Xu, A. (2020). The provenance of regolith at the Chang'e-5 candidate landing region. *Journal of Geophysical Research: Planets*, *125*(5), e2019JE006112. https://doi.org/10.1029/2019JE006112

Zhang, D., Su, B., Chen, Y., Yang, W., Mao, Q., & Jia, L. H. (2022). Titanium in olivine reveals low-Ti origin of the Chang'E-5 lunar basalts. *Lithos*, *414–415*, 106639. https://doi.org/10.1016/j.lithos.2022.106639

Zong, K., Wang, Z., Li, J., Hea, Q., Li, Y., Becker, H., et al. (2022). Bulk compositions of the Chang'E-5 lunar soil: Insights into chemical homogeneity, exotic addition, and origin of landing site basalts. *Geochimica et Cosmochimica Acta*, *335*(335), 284–296. https://doi.org/10.1016/j.gca.2022.06.037